

COMPARATIVE INVESTIGATION OF ULTRASONIC CAVITATION EROSION FOR TWO ENGINEERING MATERIALS

T. Volkov-Husović ^a, S. Martinović ^b, A. Alil ^{b,*}, M. Vlahović ^b, B. Dimitrijević ^c, I. Ivanić ^d, V. Pavkov ^e

^a University of Belgrade, Faculty of Technology and Metallurgy, Belgrade, Serbia

^b University of Belgrade, Institute of Chemistry, Technology and Metallurgy - National Institute of the Republic of Serbia, Belgrade, Serbia

^c University of Belgrade, Faculty of Mining and Geology, Belgrade, Serbia

^d University of Zagreb, Faculty of Metallurgy, Sisak, Croatia

^e University of Belgrade, Vinča Institute of Nuclear Sciences - National Institute of the Republic of Serbia, Belgrade, Serbia

(Received 18 January 2024; Accepted 19 September 2024)

Abstract

Engineering materials are often exposed to various extremely harsh environments such as high temperatures and/or high pressure, thermal shocks, aggressive solutions, or cavitation erosion. The phenomenon of cavitation erosion is to be expected with flowing fluids where the parts of equipment include turbine blades, high-speed propellers, or pump parts. Such conditions usually cause surface degradation with defects in the form of pits and fractures, resulting in strength deterioration with a potential risk of failure, as well as shortening the lifespan of the materials requiring additional expenses for failure analysis, repair, and/or replacement of parts. This paper presents the main results of the cavitation erosion resistance study of two different engineering materials, 316L austenitic stainless steel and CuAlNi shape memory alloy (SMA). The cavitation erosion testing was carried out using an ultrasonic vibratory method with a stationary sample. The comparison of the behavior of these two materials under cavitation erosion conditions is shown based on the results of mass loss and analysis of the pits formed over time. Image analysis tools were used to quantify the surface damage levels. Detailed analyses revealed that the CuAlNi shape memory alloy (SMA) exhibited superior in terms of resistance and better behavior compared to stainless steel.

Keywords: Cavitation erosion; 316L steel; CuAlNi SMA; Image analysis

1. Introduction

The most commonly used standard procedure for determining material resistance to cavitation erosion is the ASTM G32-16 test method. The cavitation erosion induced by ultrasonic waves involves the transmission of sound waves within the ultrasonic frequency spectrum, which equals or exceeds 20 kHz, through a liquid medium. The “cavities in the liquid” or bubbles form and grow when negative pressure amplitude drops to or below the vapor pressure of the liquid. Subsequently, these bubbles collapse during the cycle of positive pressure generating high-pressure shockwaves and microjets [1, 2]. More precisely, the bubbles formed in low-pressure regions are filled with vapor or dissolved gases that implode after their formation, which can be very violent in higher pressure areas. During the implosion of the bubbles, micro-jets and shock waves are generated.

Their repeated impacts can cause mass loss of material – a phenomenon known as cavitation erosion. The mass loss together with formed cavities reduces the lifetime of the materials and/or equipment, raising maintenance costs and can lead to catastrophic collapse [3-6].

There are two main mechanisms of cavitation erosion, the formation of shock waves (I and II) and microjet (III and IV), as shown in Figure 1. The subsequent impact of microjet and shock wave eventually led to the formation of pits [3-6]:

- If the cloud of bubbles collapses, a shock wave is emitted into the fluid (I and II); the magnitude of the shock wave weakens as it moves towards the solid surface;

- If the bubble collapses close enough to the solid surface, a micro-jet phenomenon occurs (III and IV); the damage in the form of a single pit is caused by a high-velocity microjet impacting the solid surface.

Corresponding author: ana.alil@ihm.bg.ac.rs

<https://doi.org/10.2298/JMMB240118018V>



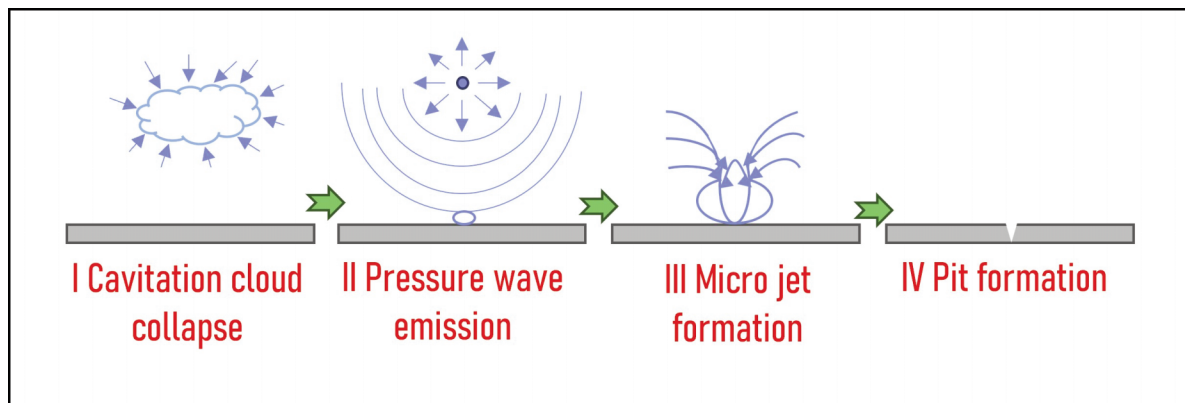


Figure 1. Schematic view of microjet and shock wave formations and their effects [4-6]

The material resistance to cavitation erosion can be graphically presented by the curves of mass/volume loss, or erosion rate during the exposure period (Figure 2 according to ASTM G32-16 [5]). Four different consecutive periods describe the overall cavitation erosion process:

I An incubation period, during which the material deforms either elastically or plastically and some micro-cracks may form, but there is no measurable mass loss;

II An acceleration period that is associated with an increasing rate of mass loss due to the propagation of cracks in the area under the cavitation impact load;

III An attenuation period in which the rate of material loss decreases;

IV A steady-state period in which the erosion rate is substantially constant.

Different metallic and non-metallic materials are impacted by cavitation during their practical applications. Understanding the material response can help to develop new structures or coatings with better cavitation resistance, which is crucial for prolonging their service life.

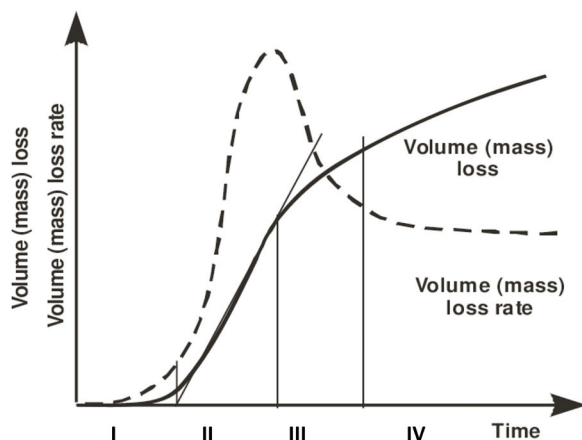


Figure 2. Cavitation curve with periods of degradation [4-6]

Metallic materials such as stainless steel and shape memory alloys (SMAs) are widely used in electronics, machinery, energetics, aerospace, civil engineering, the automotive industry, medicine, and daily life [7, 8].

Because of its good corrosion and cavitation resistance, 316L austenitic stainless steel is commonly used in hydraulic machinery such as pumps and pipes [9-11]. Therefore, the cavitation erosion behavior of 316L stainless steel, processed by selective laser melting, was chosen to test in this study [12, 13]. 316L stainless steel is the second most frequently used austenitic stainless steel, also known as marine-grade stainless steel since it is mainly used for the manufacture of ship propellers. It is a low-carbon stainless steel with a density of 7.9 g/cm^3 and the main alloying elements of Cr, Ni, and Mo with a small percentage of Si and P.

The cavitation erosion behavior of 316L stainless steel, processed by selective laser melting (SLM), was investigated in the studies [12, 13]. The aim was to observe the mechanisms and morphology of the damage as well as the microstructure-related cavitation erosion resistance of SLM-densified 316L steel. Other authors were interested in the combination of cavitation erosion of 316L steel with corrosion in NaCl solution [13] and cavitation resistance of a distillation column made of 316L stainless steel for food industry applications [14, 15].

A shape memory alloy (SMA) is often described as an alloy that “remembers” its original, cold-forged shape; it returns to the pre-deformed shape when heated. The main types of SMAs are nitinol (Ni-Ti), Cu-based, and Fe-based alloys. Considering all material characteristics, Cu-based alloys are the most commercial of the SMA group. Compared to other shape memory alloys, Cu-based SMAs are produced by relatively simple fabrication procedure and have higher electrical and thermal conductivity. The economic effect (low price) is the main advantage of

Cu-based SMAs compared with other SMAs. Owing to their properties, including excellent thermal stability and high transformation temperatures (close to 200 °C), Cu-Al-Ni SMAs can be applied in various industries, such as medical and aerospace. This exceptional class of materials can be used as a lightweight, solid-state replacement for conventional actuators such as hydraulic, pneumatic, and motor-based systems [16-21].

The cavitation erosion of SMAs was tested primarily for nitinol alloys and Fe-based and nitinol SMAs [22-26]. The reported results indicate good cavitation resistance of Fe-Mn-Si-Cr SMAs [23] and Ni-Ti SMAs, which were used as cavitation resistant coatings [23].

The results of investigating the surface morphology and grain structure of cavitation tested CuZnAl SMA pointed out that under the cavitation impact grains are refined and their orientations are diversified, the transformation of martensite to austenite is facilitated, and the stability of thermoelastic martensite decays, which presents the improvement of shape memory performance [27, 28].

This paper aims to deal with damage monitoring during the cavitation process using software tools for image analysis to quantify morphological parameters that are selected as the best ones to describe induced pits and defects. The motivation of the research presented here is to predict as precisely as possible the response of the selected material surface to a highly unsteady fluid flow, as occurs during cavitation exposure in order to mitigate its effects on submerged bodies.

2. Experimental

2.1. Materials

In this experiment, the commercial stainless steel powder of the grade Surfit™ 316L was used. The chemical composition of the stainless steel Surfit™ 316L is given in Table 1. This type of stainless steel has an austenitic structure, while the defined contents of Cr, Ni, and Mo provide its significant corrosion resistance, so it can also be assumed the cavitation erosion resistance. The spherical stainless steel powder was obtained by gas atomization. Using a sieve analysis, the powder was sieved in the range of particle size range from 45 to 90 μm in diameter.

Before the pressing process, the steel powder was manually homogenized with a binder in a ceramic

mortar for 15 min. Paraffin wax, commercial name Paraplast™ [29], was used as a binder in the content of 1 wt.%. After homogenization, cold uniaxial double-sided pressing of the powder was performed to obtain cylindrical green compacts 16 mm in diameter. The samples were pressed at about 150 MPa and then sintered in a vacuum into a high-temperature vacuum furnace (HBO W, GERO, Germany) at the temperature of 1200 °C for 60 min [30].

The polycrystalline Cu-12.8Al-4.1Ni (wt.%) SMA was prepared from pure raw materials of copper, aluminium, and nickel in a vacuum induction furnace. The heating temperature was 1240 °C. A solid bar of 8 mm was produced directly from the melt employing a device for the vertical continuous casting connected to a vacuum induction furnace. Continuous casting of the bar was carried out at a casting speed of 320 mm/min (as-cast state, sample L). After the casting, the heat treatment procedure was performed by solution annealing at 885 °C for 60 min followed by water quenching [32, 33]. The chemical composition is given in Table 2. Table 3 shows the major mechanical properties of both tested metallic materials [32, 33].

2.2. Methods

A schematic diagram of the part of the cavitation experimental setup is shown in Figure 3. The test was performed using the ultrasonic vibration method (with a stationary sample), according to ASTM G32-16 standard [5]. To produce cavitation bubbles, an

Table 2. Chemical composition of Cu-12.8Al-4.1Ni SMA (wt.%(wt.%) [31]

Chemical element	Cu	Al	Ni
Value (wt.%)	83.2	12.80	4.10

Table 3. Mechanical properties of stainless steel 316L and Cu-12.8Al-4.1Ni SMA

Property	Stainless steel 316L	Cu-12.8Al-4.1Ni SMA
Yield Strength, min. MPa	205	242
Tensile Strength, min. (MPa)	551	403
Elongation, min. (%)	1.64	1.64
Hardness, max. (HV0.5)	150	290.7

Table 1. Chemical composition of stainless steel 316L (wt.%) [31]

Chemical element	C	Cr	Ni	Mo	Mn	Si	Fe
Typical value (wt.%)	max. 0.03	16.0-18.0	10.0-14.0	2.0-3.0	1.0-2.0	max.1.0	Bal.



ultrasonic generator with 20 ± 0.2 kHz frequency was used. The ultrasonic horn tip diameter was 16 mm and the working distance between the horn tip and the exposed specimen surface was set to 0.5 mm. Test samples were placed on a holding platform in a beaker filled with distilled water at a temperature of 22 ± 1 °C. The specimen was placed 10 mm under the free liquid level. Samples' dimensions were a diameter of 15.5 mm and a height of 6 mm. The specimens were weighed prior to the cavitation exposure (CE) test and after each certain period of exposure. Additionally, an optical microscope was used to monitor the exposed surface with the aim of analyzing changes in damage morphology. In order to achieve the repeatability of obtained results, three specimens were used for the measurements, while each presented result is the mean value of the obtained results. The mass measurements of the test specimens during the experiment were carried out on an analytical balance with an accuracy of 0.1 mg. The test specimens were dried in a dryer at 110 °C for one hour, before being weighed.

To assess the impact of surface erosion, the

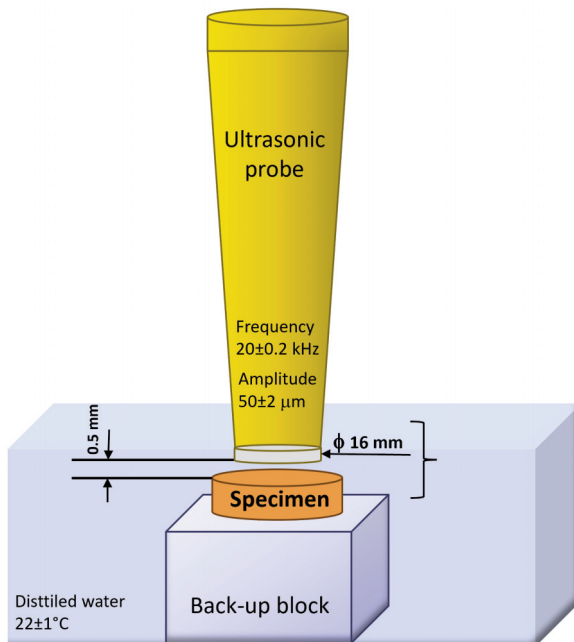


Figure 3. Schematic illustration of experimental set-up segment, vibrating tip (ultrasonic horn)

samples' surfaces were examined using a trinocular metallurgical microscope (EUME, EU Instruments, Gramma Libero, Belgrade) at various magnifications. Besides, microphotographs of the tested specimens were taken using SEM type JEOL JSM-5800 to monitor changes during CE. Microstructural characterization was performed on prepared metallographic samples: sanded with different grid sandpaper (400 - 1200), polished in an Al_2O_3 solution, and finally etched in a solution of 2.5 g FeCl_3 , 10 ml HCl and 48 ml of methanol.

Defects resulting from cavitation erosion can be characterized by morphological descriptors and be quantified using appropriate tools for image analysis in the Image Pro Plus 6.0 software (IPP) package (Media Cybernetics, 2006, Rockville, MD). The sample surface was scanned at high resolution (1200 dpi) after each specific CE period and then processed by IPP. The morphological characteristics that best characterize the extracted object were chosen after the surface defects (pits) were segmented. Then, using the software tools, a quantitative assessment of each selected descriptor is made possible, allowing for the description of induced defects and additional analysis of the data regarding their changes. During this research, selected defect descriptors were Area, $\text{Diameter}_{\text{max}}$, $\text{Diameter}_{\text{min}}$, $\text{Diameter}_{\text{mean}}$, $\text{Radius}_{\text{min}}$, and Roundness. Figure 4 provides an illustration of the parameters that were chosen to be monitored while the tested materials were exposed.

3. Results and Discussion

The structural investigations of the damaged areas were carried out using the optical microscope (OM) and scanning the exposed surface depending on the duration of repeated loads. The appearance of some stainless steel sample surfaces is presented in Figure 5.

The structure of 316L stainless steel before testing indicates that a typical sintered heterogeneous granular structure was formed. The microstructure shows abundant coarse austenite grains (γ) of different sizes and irregular shapes, as well as also pores with elongated morphology, mainly visible on the grain boundaries. It is evident that intergranular



Figure 4. Graphical presentation of selected and monitored parameters

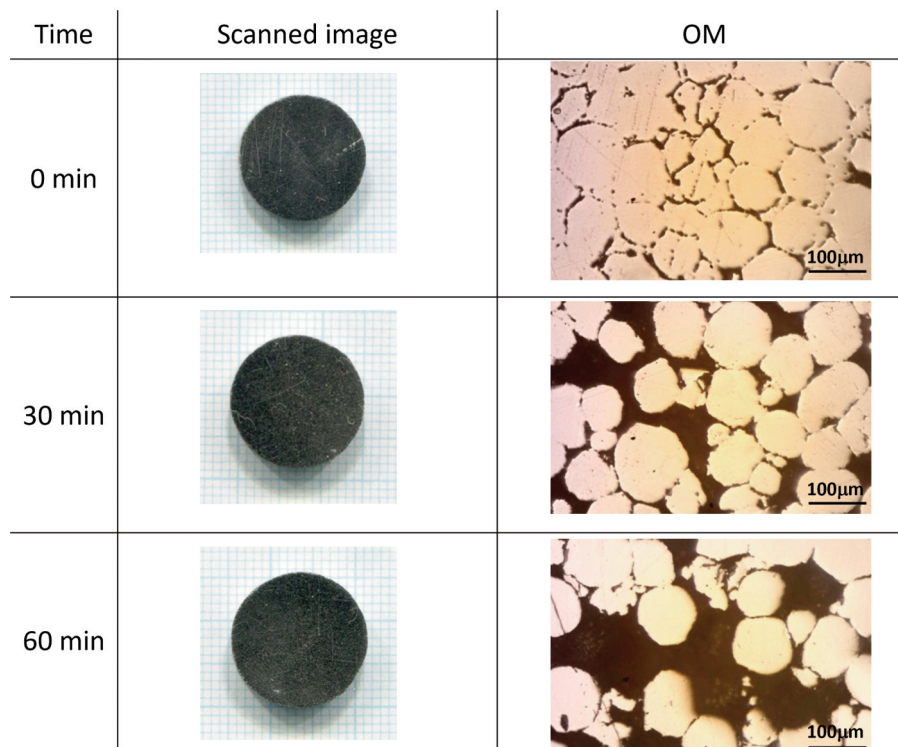


Figure 5. The images of the stainless steel 316L sample made by a scanner and an optical microscope used in additional image analysis

erosion is being caused by the degradation along the grain boundary during the cavitation testing. Namely, it can be claimed that the grain boundaries represent weak points where the material begins to degrade and then spread with the loss or erosion of the austenite grains while the portion of pores increases.

This observation is proven by measuring the mass of samples subjected to the cavitation, as recommended in the standard. Besides, additional monitoring of degradation is focused on image analysis of surfaces that had been exposed to cavitation. More precisely, morphological parameters that depict the induced defects or pits were chosen and quantified using tools of image analysis. Results of the mass loss and the total damaged surface area which is presented as the level of degradation are given in Figure 6.

By considering the results of mass loss in time, it can be noted that the incubation period almost does not exist or is nearly negligible, since in the initial 10 minutes there is measurable mass loss regardless as this is quite small and can be attributed to the second accumulation period. After 10 minutes of cavitation load, there is a steady-state period in which there is no further loss of mass. It can be claimed that the stainless steel shows excellent resistance to the cavitation since the mass loss after 60 minutes of cavitation loading did not exceed 0.03 mg while the

damage level of the sample surface did not exceed 1.75 %.

Regarding the testing of SMA samples and because of the exceptional properties that these alloys possess, the testing lasted for 420 minutes. The surface changes related to forming and growing the damages that occurred during the cavitation were on a nanoscale level so that they could only be detected by measuring the mass to the three decimal places and using techniques such as SEM and AFM methods. Figure 7 shows 3D AFM and SEM images of the SMA sample

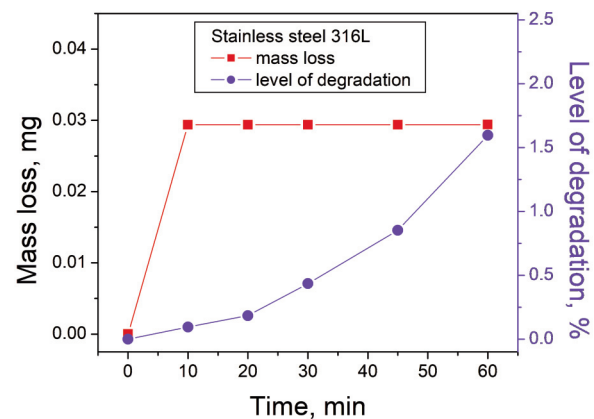


Figure 6. Mass loss and level of degradation of the stainless steel 316L sample during cavitation testing

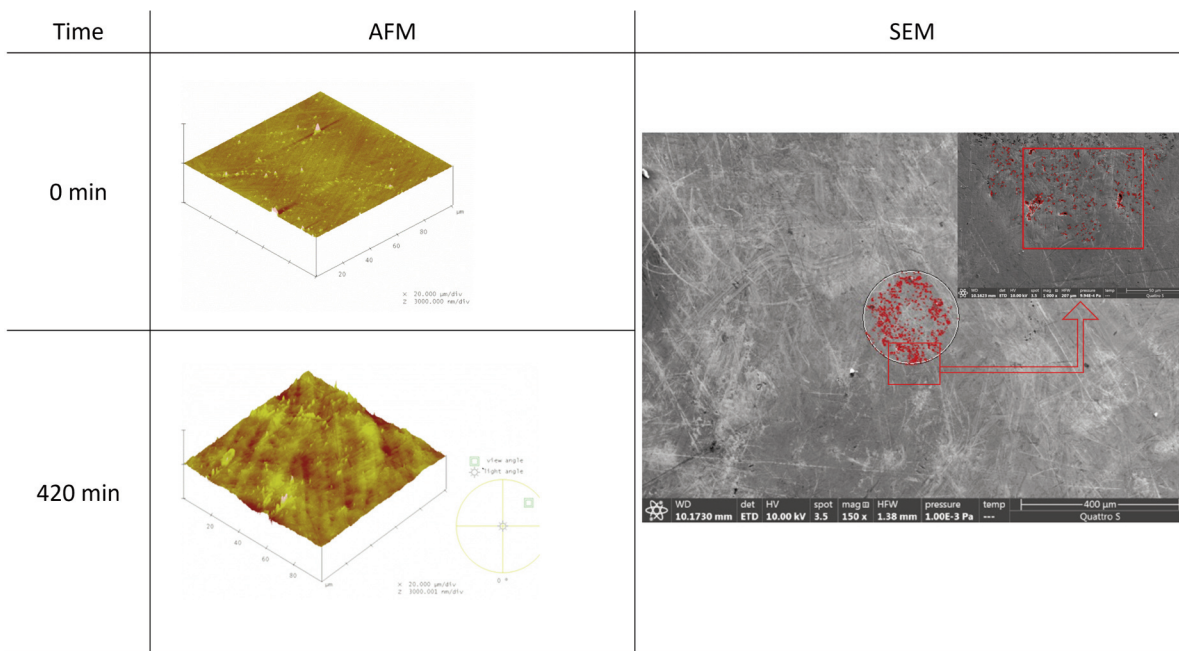


Figure 7. 3D AFM and SEM images of the CuAlNi shape memory alloy (SMA) sample surface before and after 420 minutes of testing

before and after 420 minutes of cavitation loads consisting of several repetitive impacts.

AFM and SEM analyses obviously indicate changes at the surface in the form of roughness in the case of AFM analysis and the form of induced pits observed by SEM. Comparing the measured roughness of the sample surface after 420 minutes of cavitation exposure with its value before the test revealed a difference of 53.73 nm, indicating that erosion is occurring on the sample surface. SEM micrographs were used to quantify surface defects induced at the surface as a consequence of cavitation impact. Visual observation of the SEM images taken during the test indicates that most occurred defects in the form of pits that have different sizes, shapes, and possible various depths. Based on that, the damaged areas were measured using the IPP software tools, while their total value was calculated as a percentage of the degraded area and presented as a level of degradation. The results of measuring the degradation level of the exposed surface are shown in Figure 8, as well as the results of the mass loss that occurred as a result of cavitation erosion.

After 420 minutes, which is 7 times longer exposure to the cavitation load than in the case of stainless steel, the mass loss is twice less than the mass loss in stainless steel for 60 minutes, so it can be noticed that the erosion of SMA is almost negligible and happens very slowly because the slope of the curve is quite mild. Since the level of degradation is less than 1.25 % after 420 minutes of cavitation load,

it can be considered as extremely low. Overall, it can be concluded that SMA is far more resistant to cavitation erosion than stainless steel; nevertheless, additional research is needed to monitor the occurrence and growth of surface defects during cavitation, which is covered in more detail in the discussion that follows.

Additional morphological parameter analysis was performed to achieve a comparative approach. Namely, to compare pits' characteristics, the morphological parameters that are at the same time descriptors of induced defects or pits were measured using image analysis tools. The average values of the obtained results are given in Table 4.

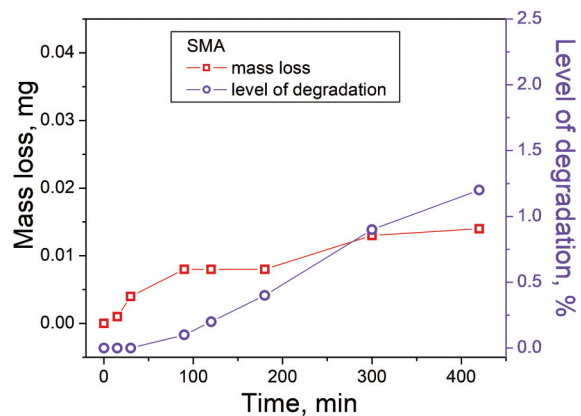


Figure 8. Mass loss and level of degradation of the CuAlNi shape memory alloy (SMA) sample during cavitation testing

Table 4. Measured average values of selected morphological parameters for the SMA after 420 min of cavitation and stainless steel 316L after 60 min of cavitation

Parameter	CuAlNi (SMA)	Steel 316L
	420 min	60 min
	Average values	
Area, μm^2	36.17	1.8
Diameter (max), μm	9.55	1.7
Diameter (min), μm	3.25	0.8
Diameter (mean), μm	6.28	1.2
Radius (min), μm	0.72	1.5
Roundness	1.25	1.65

During the analysis of obtained measurements, it should be kept in mind that the SMA sample was subjected to cavitation for 420 minutes, whereas the stainless steel was exposed for 60 minutes. Even in such conditions where the SMA sample is exposed to cavitation seven times longer than the sample of stainless steel, the results of mass loss and degradation level are very small for both materials, so it can be claimed that they both have excellent resistance to cavitation erosion. Otherwise, it should be emphasized that SMA even after 420 minutes shows lesser mass loss and degradation levels than stainless steel.

The average results of the measured values related to important parameters of induced pits show that in the case of SMA, each individual defect or pit has greater values for Area and Diameter in comparison

with the stainless steel, Table 4. This observation suggests that fewer bigger pits with larger areas occur at the surface of SMA. It should also be noted that these pits are shallow and surficial, based on the roughness values and AFM analysis. On the contrary, in the case of stainless steel, the results of these parameters indicate that a larger number of smaller pits are formed at the surface. Such differences in behavior can be attributed to the different microstructures of SMA and stainless steel, which are austenitic and martensitic, respectively. The average values of the minimal radius of an individual defect are about twice as small for SMA as they are for stainless steel, indicating that the defect is exceedingly thin and narrow in some places. The obtained average values for the roundness of induced pits that developed at the SMA surface indicate that they are more like circle shapes than those formed at the stainless sample surface since the SMA average value of roundness is closer to the value 1.

The mass loss rate could be very useful for different period determination. Based on the obtained results, the samples' mass loss rate is given in Figure 9. The sample steel 316L is characterized by a short incubation period (10 minutes) accompanied with a short accumulation period (10 to 45 minutes). The attenuation period is achieved in 45 minutes. Further experiments could lead to achieving a steady state period. Different results were obtained for CuAlNi SMA samples. The incubation period was similar (30 minutes), but the accumulation period was much longer (up to 200 min), and the attenuation period after that time of exposure.

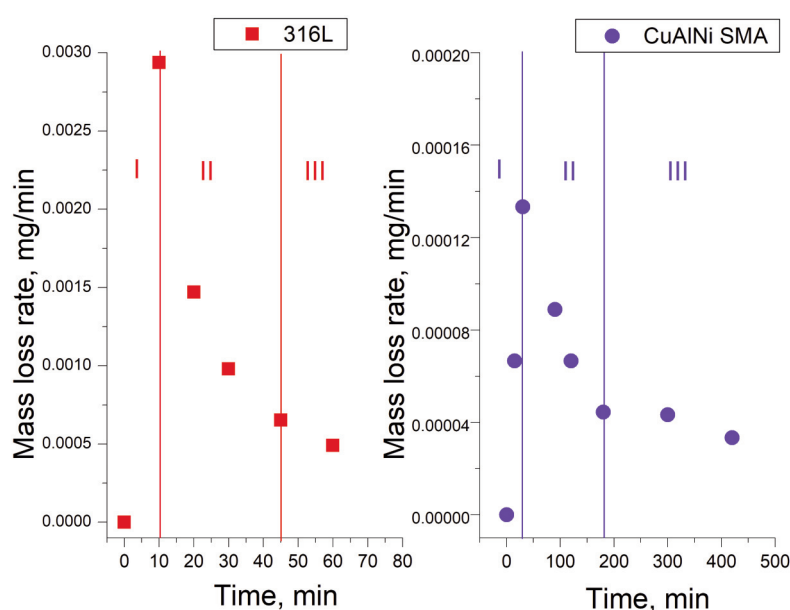


Figure 9. The mass loss rate of the 316L steel and CuAlNi shape memory alloy (SMA) sample during cavitation testing



4. Conclusions

The presented investigation involved the examination of the cavitation erosion resistance of two metallic engineering materials. The determination of mass loss and levels of surface degradation was carried out during the testing process. Furthermore, the measurement and analysis of various selected morphological parameters of defects induced by the cavitation load were conducted using image analysis software tools.

The obtained results allow the following conclusions to be drawn:

- In terms of mass loss, it was observed that both materials exhibited excellent resistance to cavitation erosion, as the decrease in mass was negligible in these samples.
- Exceptional resistance to cavitation erosion is also indicated by the measured levels of degradation which are very low at 1.5 % and 1.25 % for the stainless steel and CuAlNi SMA samples, respectively.
- It should be emphasized that similar results of mass loss and degradation level for both tested materials were obtained; however, since the duration of cavitation exposure exceeded 420 minutes, it is evident that the CuAlNi SMA sample exhibited a higher degree of cavitation erosion resistance in comparison to the sample of stainless steel.
- The average measured values of selected morphological parameters representing each defect or pit indicate the following findings: fewer shallow pits with larger areas occur at the surface of CuAlNi SMA, whereas a greater number of smaller and deeper pits are formed at the surface of stainless steel, the pits on the CuAlNi SMA surface indicate that they are more circular than those formed on the stainless steel sample. These differences can be attributed to the dissimilar microstructures of CuAlNi SMA and stainless steel.
- Mass loss rate diagrams pointed out differences in the cavitation periods for samples. The CuAlNi SMA sample exhibited longer times for each period of cavitation. The largest difference was in the duration of the attenuation period.
- According to the results obtained and previous analysis, both materials can be considered reliable candidates for application in cavitation erosion conditions, despite the large differences in the examined materials.

Acknowledgments

This work was financially supported by the Ministry of Science, Technological Development and

Innovation of the Republic of Serbia (Contract Nos. 451-03-65/2024-03/200135, 451-03-66/2024-03/200026 and 451-03-47/2023-01/200017).

Author Contributions

T. Volkov-Husović: Conceptualization, Methodology, Software, Formal analysis, Writing-original draft preparation, Writing-review and editing, Supervision.

S. Martinović: Methodology, Formal analysis, Writing-original draft preparation, Writing-review and editing, Supervision.

A. Alil: Methodology, Formal analysis, Writing-original draft preparation, Writing-review and editing, Supervision.

M. Vlahović: Methodology, Formal analysis, Writing-original draft preparation, Writing-review and editing, Supervision.

B. Dimitrijević, Writing-review and editing, Supervision.

I. Ivanić: Materials synthesis and characterization
V. Pavkov: Materials synthesis and characterization, Supervision

All authors have read and agreed to the published version of the manuscript.

Data availability

No data were used for the research described in the article.

Conflict of interest

The authors declare that they have no known competing financial interests or personal relationships that could have appeared to influence the work reported in this paper.

References

- [1] F.G. Hammit, Cavitation and multiphase flow phenomena; McGraw-Hill, New York, 1980.
- [2] T.J.C. van Terwisga, P.A. Fitzsimmons, L. Ziru, E.-J. Foeth, Cavitation erosion - A review of physical mechanisms and erosion risk models, 2009. <http://resolver.tudelft.nl/uuid:e1c525da-e944-4d4a-b440-d324b3e382cf>
- [3] K.L. Tan, S.H. Yeo, Cavitation erosion study in deionized water containing abrasive particles, Proceedings 26th International DAAAM Symposium, 21-24th October, Zadar, Croatia, 2016, pp. 818-824.
- [4] G.L. Chahine, J.-P. Franc, A. Karimi, Advanced experimental and numerical for cavitation erosion prediction, Springer International Publishing, Dordrecht, 2014.
- [5] ASTM G32-16; Standard test method for cavitation



- erosion using vibratory apparatus. ASTM International: West Conshohocken, PA, USA, 2021.
- [6] D.E. Zakrzewska, A.K. Krella, Cavitation erosion resistance influence of materials properties, *Advances in Materials Science*, 19 (4) (2019) 18-34. <https://doi.org/10.2478/adms-2019-0019>
- [7] E. Clithy, Application of shape memory alloy, *Science Insight*, 33 (3) (2020) 167-174. <http://dx.doi.org/10.2139/ssrn.3614161>
- [8] Available online: <https://www.totalmateria.com/page.aspx?ID=CheckArticle&site=kts&LN=TH&NM=439> (accessed on 25 December 2023).
- [9] G. Gao, Z. Zhang, Cavitation erosion behavior of 316L stainless steel, *Tribology Letters*, 67 (2019) 112. <https://doi.org/10.1007/s11249-019-1225-0>
- [10] L. Zhen, J. Han, J. Lu, J. Chen, Cavitation erosion behavior of Hastelloy C-276 nickel-based alloy, *Journal of Alloys and Compounds*, 619 (2015) 754-759. <https://doi.org/10.1016/j.jallcom.2014.08.248>
- [11] F.T. Cheng, C.T. Kwok, H.C. Man, Cavitation erosion resistance of stainless steel laser-clad with WC-reinforced MMC, *Materials Letters*, 57(4) (2002) 969-974. [https://doi.org/https://doi.org/10.1016/S0167-577X\(02\)00907-2](https://doi.org/https://doi.org/10.1016/S0167-577X(02)00907-2).
- [12] H. Ding, Q. Tang, Y. Zhu, C. Zhang, H. Yang, Cavitation erosion resistance of 316L stainless steel fabricated using selective laser melting, *Friction*, 9 (6) (2021) 1580-1598. <https://doi.org/10.1007/s40544-020-0443-7>
- [13] C. Harges, F. Pöhl, A. Röttger, M. Thiele, W. Theisen, C. Esen, Cavitation erosion resistance of 316L austenitic steel processed by selective laser melting (SLM), *Additive Manufacturing*, 29 (7) (2019) 100786. <https://doi.org/10.1016/j.addma.2019.100786>
- [14] J. Hu, L. Zhang, A. Ma, P. Mao, Y. Zheng, Effect of cavitation intensity on the cavitation erosion behavior of 316L stainless steel in 3.5 wt.%NaCl solution, *Metals*, 12 (2022) 198. <https://doi.org/10.3390/met12020198>
- [15] E. Proverbio, L.M. Bonaccorsi, Erosion-corrosion of a stainless steel distillation column in food industry, *Engineering Failure Analysis*, 9 (6) (2002) 613-620. [https://doi.org/10.1016/S1350-6307\(02\)00027-4](https://doi.org/10.1016/S1350-6307(02)00027-4)
- [16] P. Kumar, S. Kumar, Shape memory alloy (SMA) a multi purpose smart material, *National Conference on Synergetic Trends in engineering and Technology (STET-2014) International Journal of Engineering and Technical Research, Special Issue* (2014) 282-285.
- [17] M.-S. Kim, J.-K. Heo, H. Rodrigue, H.-T. Lee, S. Pané, M.-W. Han, S.-H. Ahn, Shape memory alloy (SMA) actuators: The role of material, form, and scaling effects, *Advanced Materials*, 35 (2023) 2208517. <https://doi.org/10.1002/adma.20220851>
- [18] M.H. Wu, L.McD. Schetky, Industrial applications for shape memory, *Proceedings International Conference on Shape Memory and Superelastic Technologies*, Pacific Grove, California, 2000, pp. 171-182.
- [19] H. Bhadeshia, R. Honeycombe, in *Stainless Steel* (H. Bhadeshia, R. Honeycombe, *Steels: Microstructure and Properties* (4th Edition), Butterworth-Heinemann, 2017, pp. 343-376. <https://doi.org/10.1016/B978-0-08-100270-4.00012-3>.
- [20] A. C. Kneissl, E. Unterweger, M. Bruncko, G. Lojen, K. Mehrabi, H. Scherngell, Microstructure and properties of NiTi and CuAlNi shape memory alloys, *Metalurgija*, 14 (2008) 89-100. <http://www.metalurgija.org.rs/mjom/vol14/No%202/2KNEISSL.pdf>
- [21] S. Kožuh, M. Gojić, I. Ivanić, T. Holjevac Grgurić, B.Kosec, I. Anžel, The effect of heat treatment on the microstructure and mechanical properties of Cu-Al-Mn shape memory alloy, *Kemijska Industrija*, 67 (1-2) (2018) 11-17.
- [22] Z. Wang, Z. Jinhua, Cavitation erosion of Fe-Mn-Si-Cr shape memory alloys, *Wear*, 256 (1) (2004) 66-72. [https://doi.org/https://doi.org/10.1016/S0043-1648\(03\)00393-4](https://doi.org/https://doi.org/10.1016/S0043-1648(03)00393-4)
- [23] G. Mauer, K.-H. Rauwald, S.Y. Jung, T.E. Weirich, Cold gas spraying of nickel-titanium coatings for protection against cavitation, *Journal of Thermal Spray Technology*, 30 (1) (2021) 131-144. <https://doi.org/10.1007/s11666-020-01139-x>
- [24] F. Cheng, P. Shi, H. Man, Cavitation erosion resistance of heat-treated NiTi, *Materials Science and Engineering A*, 339 (2003) 312-317. [https://doi.org/10.1016/S0921-5093\(02\)00162-4](https://doi.org/10.1016/S0921-5093(02)00162-4)
- [25] S. Hattori, A. Tainaka, Cavitation erosion of Ti-Ni base shape memory alloys, *Wear*, 262 (2007) 191-197. <https://doi.org/10.1016/j.wear.2006.05.012>
- [26] L. Yang, A. Tieu, D. Dunne, S. Huang, H. Li, D. Wexler, Z. Jiang, Cavitation erosion resistance of NiTi thin films produced by filtered arc deposition, *Wear*, 267 (2009), 233-243. <http://dx.doi.org/10.1016/j.wear.2009.01.035>
- [27] H. Liu, J. Chen, X. Wei, C. Kang, K. Ding, Effects of cavitation on grain structure and phase transformation of CuZnAl shape memory alloy, *Journal of Applied Science and Engineering*, 24 (1) (2021) 111-121. [https://doi.org/10.6180/jase.202102_24\(1\).0015](https://doi.org/10.6180/jase.202102_24(1).0015)
- [28] M.J. Jani, M. Leary, A. Subic, M.A. Gibson, A review of shape memory alloy research, *Applications and Opportunities*, *Materials & Design*, 56 (2014) 1078-1113. <https://doi.org/https://doi.org/10.1016/j.matdes.2013.11.084>
- [29] "Paraplast™, MLS" Available online: <https://www.mls.be/en/p/paraplast/paraplast/> (accessed on 15 January 2024).
- [30] T. Volkov-Husović, S. Martinović, A. Alil, M. Vlahović, Application of image analysis for cavitation erosion monitoring of some engineering materials, *Proceedings 54th International October Conference on Mining and Metallurgy*, 18-21 October, Bor, Serbia, 2023, p. 531-534.
- [31] "Surfit™ 316L Product Data Sheet" Available online: <http://www.serfla.com.br/pdf/316L.pdf> (accessed on 15 January 2024).
- [32] T. Volkov-Husović, I. Ivanić, S. Kožuh, S. Stevanović, M. Vlahović, S. Martinović, S. Stopic, M. Gojić, Microstructural and cavitation erosion behavior of the CuAlNi shape memory alloy, *Metals*, 11 (7) (2021) 997. <https://doi.org/10.3390/met11070997>
- [33] I. Ivanić, M. Gojić, S. Kožuh, B. Kosec, Microstructural analysis of CuAlNiMn shape-memory alloy before and after the tensile testing, *Materiali in tehnologije / Materials and technology*, 48 (5) (2014) 713-718. <https://urn.nsk.hr/urn:nbn:hr:115:226928>



UPOREDNO ISPITIVANJE ULTRAZVUČNE KAVITACIONE EROZIJE DVA INŽENJERSKA MATERIJALA

T. Volkov-Husović ^a, S. Martinović ^b, A. Alil ^{b,*}, M. Vlahović ^b, B. Dimitrijević ^c, I. Ivanić ^d, V. Pavkov ^e

^a Univerzitet u Beogradu, Tehnološko-metalurški fakultet, Beograd, Srbija

^b Univerzitet u Beogradu, Institut za hemiju, tehnologiju i metalurgiju - Nacionalni institut Republike Srbije, Beograd, Srbija

^c Univerzitet u Beogradu, Rudarsko-geološki fakultet, Beograd, Srbija

^d Univerzitet u Zagrebu, Metalurški fakultet, Sisak, Hrvatska

^e Univerzitet u Beogradu, Institut za nuklearne nauke Vinča - Nacionalni institut Republike Srbije, Beograd, Srbija

Apstrakt

Inženjerski materijali često su izloženi raznim izuzetno teškim uslovima, kao što su visoke temperature i/ili visoki pritisci, termički udari, agresivnim rastvorima ili kavitacionoj eroziji. Fenomen kavitacione erozije očekuje se kod tečnosti u pokretu, gde delovi opreme uključuju lopatice turbina, propelere velike brzine ili delove pumpi. Takvi uslovi obično izazivaju degradaciju površine sa defektima u obliku udubljenja i pukotina, što rezultira smanjenjem čvrstoće i potencijalnim rizikom od kvara, kao i skraćivanjem životnog veka materijala, što zahteva dodatne troškove za analizu kvara, popravku i/ili zamenu delova. Ovaj rad predstavlja glavne rezultate studije otpornosti na kavitacionu eroziju dva različita inženjerska materijala, austenitnog nerđajućeg čelika 316L i CuAlNi legure sa efektom pamćenja oblika (SMA). Ispitivanje kavitacione erozije sprovedeno je korišćenjem ultrazvučne vibracione metode sa stacionarnim uzorkom. Poređenje ponašanja ova dva materijala u uslovima kavitacione erozije prikazano je na osnovu rezultata gubitka mase i analize udubljenja nastalih tokom vremena. Alati za analizu slike korišćeni su za kvantifikaciju nivoa oštećenja površine. Detaljne analize su pokazale da je CuAlNi legura sa efektom pamćenja oblika (SMA) pokazala superiorniju otpornost i bolje ponašanje u poređenju sa nerđajućim čelikom.

Ključne reči: Kavitaciona erozija; 316L čelik; CuAlNi SMA; Analiza slike

